

WILEY-VCH

 **Chemistry  
Europe**

European Chemical  
Societies Publishing

# Take Advantage and Publish Open Access



By publishing your paper open access, you'll be making it immediately freely available to anyone everywhere in the world.

That's maximum access and visibility worldwide with the same rigor of peer review you would expect from any high-quality journal.

**Submit your paper today.**



[www.chemistry-europe.org](http://www.chemistry-europe.org)

## Green Chemistry | Hot Paper |

## Organophotocatalytic N-Demethylation of Oxycodone Using Molecular Oxygen

Yuesu Chen,<sup>[a, b]</sup> Gabriel Glotz,<sup>[a, b]</sup> David Cantillo,<sup>\*,[a, b]</sup> and C. Oliver Kappe<sup>\*,[a, b]</sup>

**Abstract:** N-Demethylation of oxycodone is one of the key steps in the synthesis of important opioid antagonists like naloxone or analgesics like nalbuphine. The reaction is typically carried out using stoichiometric amounts of toxic and corrosive reagents. Herein, we present a green and scalable organophotocatalytic procedure that accomplishes the N-demethylation step using molecular oxygen as the terminal ox-

idant and an organic dye (rose bengal) as an effective photocatalyst. Optimization of the reaction conditions under continuous flow conditions using visible-light irradiation led to an efficient, reliable, and scalable process, producing nor-oxycodone hydrochloride in high isolated yield and purity after a simple workup.

## Introduction


Thebaine (**1**) is one of the naturally occurring opiate alkaloids.<sup>[1]</sup> It is extracted from *Papaver bracteatum* (Iranian poppy), in which it can be found in large abundance (up to 26% wt. of dried latex, 98% wt. of total alkaloids).<sup>[2]</sup> Thebaine is utilized as a starting material for the synthesis of several drugs. The most well-known analgesic synthesized from thebaine is oxycodone (**2**), which is produced over two synthetic steps (Scheme 1A) and is widely used in clinics to alleviate severe pain caused by surgeries or cancers.<sup>[3]</sup> Overdose of opioid analgesics gives rise to respiratory depression and death.<sup>[4]</sup> Naloxone (**4a**), a short-acting opioid antagonist, has been used for the treatment of acute poisoning of narcotic opioids since the 1960s.<sup>[5]</sup> As this relatively inexpensive medication can completely reverse the effects of opioid overdose,<sup>[6]</sup> naloxone is included in the World Health Organization's *Model List of Essential Medicines*.<sup>[7]</sup> Naloxone can be prepared from oxymorphone by replacing the N-methyl by an N-allyl group, with oripavine as the naturally oc-


curing starting material.<sup>[8]</sup> However, the natural abundance of oripavine (up to 1.5 wt% of dried latex of *P. orientale*, or 27 wt% of total alkaloids) is much lower than thebaine.<sup>[9]</sup> Thus, the synthesis from thebaine via oxycodone **2** is an attractive alternative (Scheme 1A). In this case, the synthetic route also includes an O-demethylation step with BBr<sub>3</sub> at room temperature.<sup>[10]</sup> In both approaches (from thebaine or oripavine), the key intermediates are the so-called nor-compounds (noroxycodone **3** and noroxymorphone **3a**), which are prepared by the N-demethylation. Indeed, the following N-functionalization provides a facile route not only to naloxone, but also to other important medicines such as nalbuphine (**4c**) by varying the alkylating agent.<sup>[11]</sup>

There are many methods for the N-demethylation of alkaloids. Only a few of them are applied for 14-hydroxy opioids.<sup>[12]</sup> Traditionally, N-demethylation is accomplished by refluxing the substrate solution with more than five equivalents of chloroformate over several hours (Scheme 1B), resulting in the nor-compounds with moderate to good yields after hydrolysis.<sup>[13]</sup> Cyanogen bromide (BrCN) can also demethylate opioids after protection of the hydroxyl groups (von Braun reaction).<sup>[14]</sup> These electrophile-based methods require the use of extremely corrosive and toxic reagents in large excess, generating a considerable amount of hazardous waste, limiting their wider practical use. More recently, several oxidative N-demethylation methods have been explored.<sup>[12]</sup> These catalytic reactions typically allow the use of green reagents such as H<sub>2</sub>O<sub>2</sub><sup>[15]</sup> and O<sub>2</sub><sup>[16]</sup> as stoichiometric oxidants. In 2008, Hudlicky and co-workers developed a palladium-catalyzed acylative N-demethylation of morphine-type alkaloids using air or O<sub>2</sub> as the oxidant (Scheme 1B).<sup>[16–17]</sup> Recently, our research group found that in situ generated palladium nanoparticles (Pd(NP)) can catalyze the N-demethylation of 14-hydroxy opioids via an 1,3-oxazolidine intermediate (e.g. **5a**) without using acid anhydrides or O-acyl protection (Scheme 1B).<sup>[18]</sup> Oxazolidine **5a** was generated via intramolecular nucleophilic addition of the 14-hydroxy group to the imini-

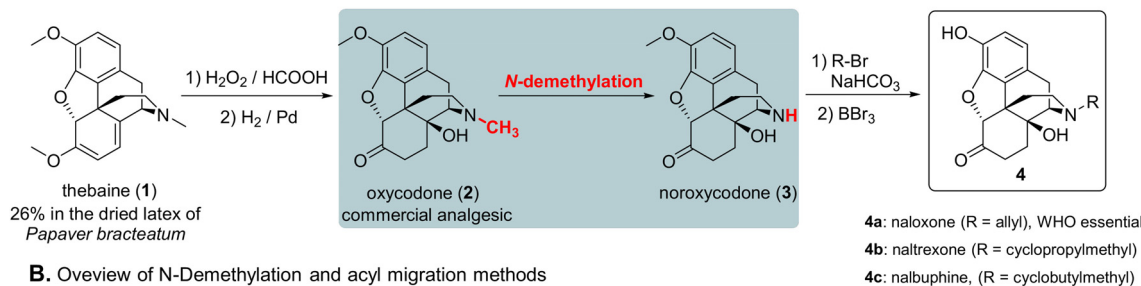
[a] Y. Chen, G. Glotz, Dr. D. Cantillo, Prof. Dr. C. O. Kappe  
Center for Continuous Flow Synthesis and Processing (CC FLOW)  
Research Center Pharmaceutical Engineering GmbH (RCPE)  
Inffeldgasse 13, 8010 Graz (Austria)  
E-mail: david.cantillo@uni-graz.at  
oliver.kappe@uni-graz.at

[b] Y. Chen, G. Glotz, Dr. D. Cantillo, Prof. Dr. C. O. Kappe  
Institute of Chemistry, University of Graz  
Heinrichstrasse 28, 8010 Graz (Austria)  
E-mail: david.cantillo@uni-graz.at  
oliver.kappe@uni-graz.at

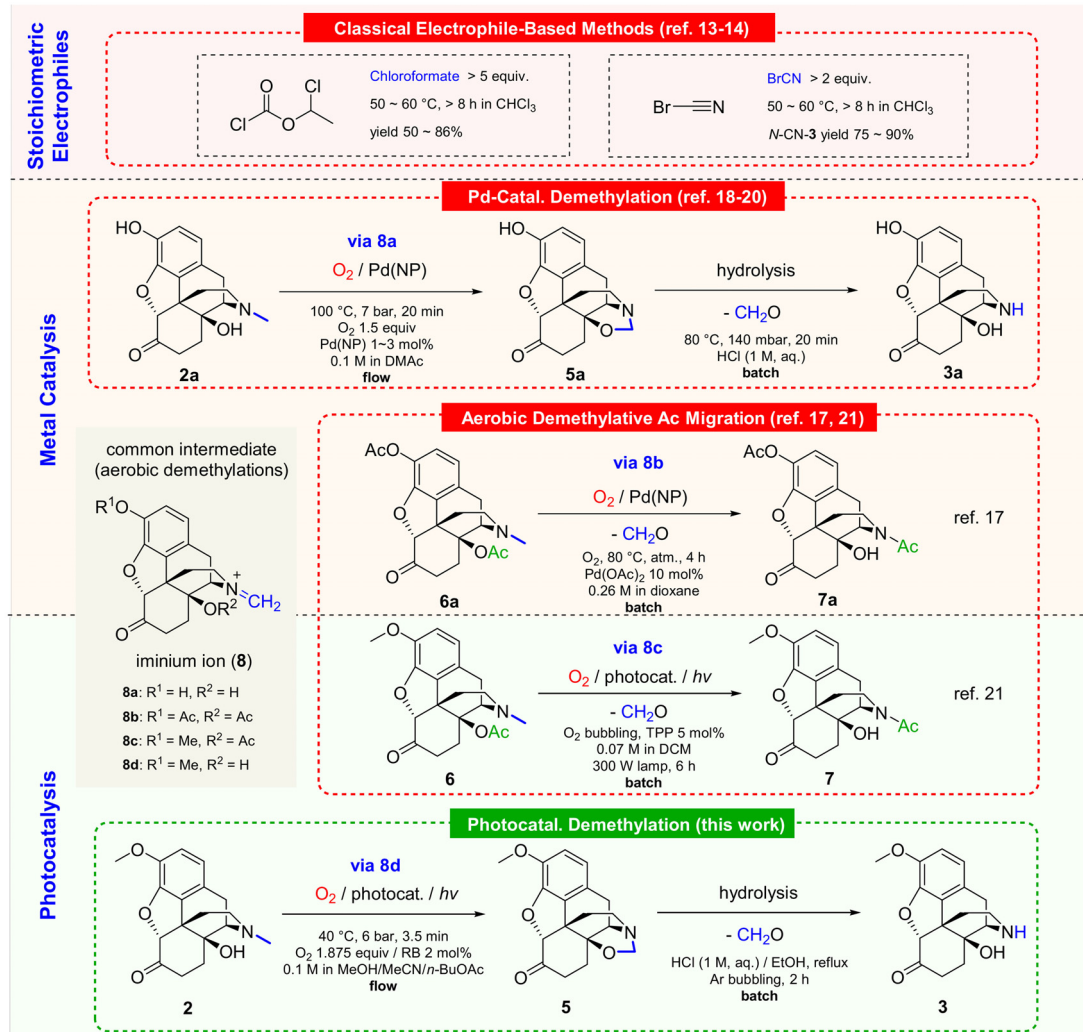
 The ORCID identification number(s) for the author(s) of this article can be found under:  
<https://doi.org/10.1002/chem.201905505>.

 © 2020 The Authors. Published by Wiley-VCH Verlag GmbH & Co. KGaA. This is an open access article under the terms of the Creative Commons Attribution Non-Commercial NoDerivs License, which permits use and distribution in any medium, provided the original work is properly cited, the use is non-commercial and no modifications or adaptations are made.

**A. Significance of N-demethylation in the synthesis of naloxone (4a) and other semisynthetic opioids**



**B. Overview of N-Demethylation and acyl migration methods**



**Scheme 1.** Significance of N-demethylation in the synthesis of semisynthetic opioids and common methods.

um electrophile in intermediate **8a** (Scheme 1B). Its O-protected counterpart **8b** was postulated as an intermediate for the N-demethylative acyl migration by Hudlicky (Scheme 1B).<sup>[17]</sup>

Methods using microreactors for the Pd-catalyzed N-demethylation of unprotected<sup>[18-19]</sup> and 3,14-O-protected<sup>[20]</sup> oxycodone (**2a**) were successively developed, enabling the reliable and safe preparation of noroxycodone (**3a**) on a kilogram scale.<sup>[20]</sup> Despite the good isolated yield ( $\approx 70\%$ ) and high productivity, the O<sub>2</sub>/Pd(NP) procedure requires a precious noble metal catalyst and elevated temperatures (120 °C). In this context, an even more sustainable and economic N-demethylation

procedure for 14-hydroxy-opioids under mild condition using environmentally friendly solvents and oxidants is highly desirable.

In 2001, Scammells and co-workers reported a photochemical N-demethylation method for some polycyclic alkaloids.<sup>[21]</sup> The proposed mechanism for the successful examples involved an iminium ion intermediate (**8**) generated through a single-electron transfer (SET)—proton transfer (PT)<sup>[22]</sup> process, which subsequently decomposed to the secondary amine and formaldehyde. The authors also observed N-demethylative acetyl migration of 14-O-acetyl oxycodone (**6**) catalyzed by tetra-

nylporphyrin (TPP), furnishing *N*-acetyl noroxycodone (**7**) in 34% yield along with an oxidation product after 6 h irradiation with a 300 W incandescent lamp in an O<sub>2</sub> atmosphere (Scheme 1B). However, their attempt to demethylate unprotected oxycodone (**2**) failed. Based on our experience with Pd-catalyzed *N*-demethylations involving iminium intermediates (**8a**),<sup>[18–20]</sup> we postulated that the reaction, in principle, should be feasible, although leading to an oxazolidine product (**5**) (Scheme 1B). Compared to the O<sub>2</sub>/Pd *N*-demethylation method, a photochemical approach would enable the reaction to be performed at room temperature using photons as a green energy source and eliminate the necessity to employ a noble metal catalyst. Moreover, mass<sup>[23]</sup>- and photon<sup>[24]</sup>-transfer limitations and safety issues associated with the use of molecular oxygen in batch reactors<sup>[25]</sup> could be overcome by using a continuous flow photochemical setup.

Herein, a continuous flow procedure for the photochemical *N*-demethylation of oxycodone (**2**) is presented (Scheme 1B). The method is based on the generation of an iminium intermediate (**8d**) by means of photoredox catalysis using molecular oxygen as the terminal oxidant. Rose bengal has been employed as an inexpensive and readily available photocatalyst. The reaction conditions were optimized and scaled utilizing a commercial flow photoreactor equipped with visible light LEDs as the irradiation source. An isolation procedure was developed to afford noroxycodone hydrochloride (**3**·HCl) in good yield and purity (Scheme 1B).

## Results and Discussion

### Catalyst screening and mechanistic investigations.

Our study began with a series of batch experiments to establish the optimal photoredox catalyst and other reaction conditions for the demethylation reaction (Table 1). LEDs with emission wavelengths of 425, 455, or 515 nm were utilized as a light source. The wavelengths were selected to match the absorption maxima of the catalysts. In the catalyst screening experiments, a solution of oxycodone (**2**) (0.05 M) and catalyst (2 mol%) in DMF (1.5 mL) was irradiated for 1 h whilst bubbling O<sub>2</sub> through the solution. Then, an aliquot of the reaction mixture was analyzed by HPLC-UV using an acetic anhydride derivatization method (see the Supporting Information for details).<sup>[18]</sup> Notably, xanthene dyes exhibited the best selectivities towards the formation of **5** (entries 7–8). Dyes containing more heavy atoms, i.e., eosin Y (EY) and rose bengal (RB) provided the highest yields (heavy atom effect; see Scheme S1 in Supporting Information). Interestingly, high conversions were achieved by catalysts featuring high intersystem crossing efficiency ( $\phi_{ISC}$ ), most of which are also potent singlet oxygen (<sup>1</sup>O<sub>2</sub>) sensitizers. Yet, side-products resulting from degradation by <sup>1</sup>O<sub>2</sub> were not observed. Instead, other reactive oxygen species (ROS), in particular, hydrogen peroxide which is formed during the reaction (vide infra), provoked degradation of the organic compounds. Other photocatalysts, such as triphenylporphyrin (TPP), 2,4,5,6-tetra(9*H*-carbazol-9-yl)isophthalonitrile (4CzIPN), or the typical [Ru(bpy)<sub>3</sub>Cl<sub>2</sub>] provided good conversions but

Table 1. Catalyst screening in batch.<sup>[a]</sup>

Entry	Cat. ( $\lambda_{max}$ [nm])	LED <sup>[b]</sup>	Comments	Conv. [%] <sup>[c]</sup>	Yield <b>5</b> [%] <sup>[c]</sup>
1	TPP (419)	425		99	57
2	Rh6G (524)	515		40	23
3	DCA (422)	425		85	14
4	4CzIPN (425)	425		99	11
5	Ru(bpy) <sub>3</sub> Cl <sub>2</sub> (453)	455		99	43
6	EB (517)	515		44	29
7	EY (520)	515		98	78
8	RB (549)	515		99	73
9	RB (549)	515	CBr <sub>4</sub> as oxidant <sup>[d]</sup>	37	24
10	RB (549)	515	CBrCl <sub>3</sub> as oxidant <sup>[d]</sup>	40	28
11	RB (549)	515	no oxidant <sup>[e]</sup>	–	–
12	RB (549)	515	no light <sup>[f]</sup>	–	–

[a] Conditions: **2** (0.05 M) + photocatalyst (2 mol%) in DMF (1.5 mL), O<sub>2</sub> (3.0 mL min<sup>-1</sup>). [b] Irradiation wavelength of the LED utilized. [c] Determined by calibrated HPLC. [d] 1 and 10 equiv of halogenated oxidant were evaluated. The reaction mixture was purged with Ar. [e] The solution was purged with Ar instead of O<sub>2</sub> under irradiation. [f] The reaction vial was wrapped with aluminum foil.

poor selectivities (selectivity refers to the HPLC peak area of the desired product with respect to the sum of all peaks except the starting material) (Table 1, entries 1, 3, 4 and 5). The poor performance observed for the other photocatalysts could be explained by the electronic properties of their excited states in some cases. 4CzIPN (entry 4), for example, is a relatively strong oxidant  $E(^3\text{cat}^*/\text{cat}^-) = +1.35$  V (vs. SCE)<sup>[26]</sup> which may account for the low selectivity obtained. 9,10-Dicyanoanthracene (DCA) (entry 3) exhibits a large singlet–triplet gap ( $\Delta E_{ST} = 1.09$  eV)<sup>[27]</sup> but a very low ISC efficiency ( $\phi_{ISC} = 0.0085$ )<sup>[28]</sup> compared to the xanthene dyes, which might also point to a reduced selectivity. Remarkably, when organic halides (CBr<sub>4</sub> and BrCCl<sub>3</sub>)<sup>[29]</sup> were used as oxidants instead of O<sub>2</sub> (entries 9 and 10), relatively low conversions were achieved, even after adding 10 equivalents of the halogenated reagents. No improvement was achieved under the same conditions using Et<sub>3</sub>N as the additive to neutralize the HBr generated during the reaction (see Figures S18 and S19 in the Supporting Information). As expected, the reaction did not proceed in the absence of light or oxygen (entries 11 and 12). Eosin Y and RB delivered analogous results. RB was selected as the catalyst for further optimizations due to its higher ISC efficiency and better solubility in some solvents.

Using RB as the catalyst, a comparison of the reaction rate at different temperatures was carried out. For this purpose, the same batch setup as described for Table 1, equipped with a transparent water jacket for temperature control, was utilized. A solution of **2** (0.1 M) and RB (2 mol%) in DMF (1.5 mL) was irradiated over 35 min whilst bubbling O<sub>2</sub> through the solution. Temperatures ranging from 10 to 60 °C were evaluated. The re-

action mixture was monitored by HPLC analysis. As expected, no significant temperature effects on the reaction rate were observed, which is common for photocatalytic reactions. The Stern–Volmer relationship for RB using **2** as a quencher resulted in a curved  $F_0/F$  vs.  $[2]$  plot (Figure 1), indicating the existence of more than one kinetically different quenching site. The data also suggested a diffusion-controlled quench, as less viscous solvents proved to be more effective (MeOH > EtOH > *n*-PrOH). An additional control experiment using the triplet quencher azulene (10 mol%) as additive inhibited the formation of **5**. These results support the assumption that the electron transfer takes place with RB in its triplet state ( $\tau = 150 \mu\text{s}$ ), and explain that catalysts with high  $\phi_{\text{ISC}}$  values exhibited the best performance.

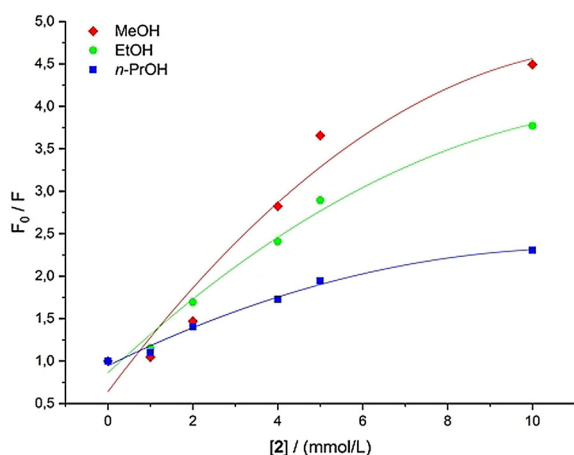
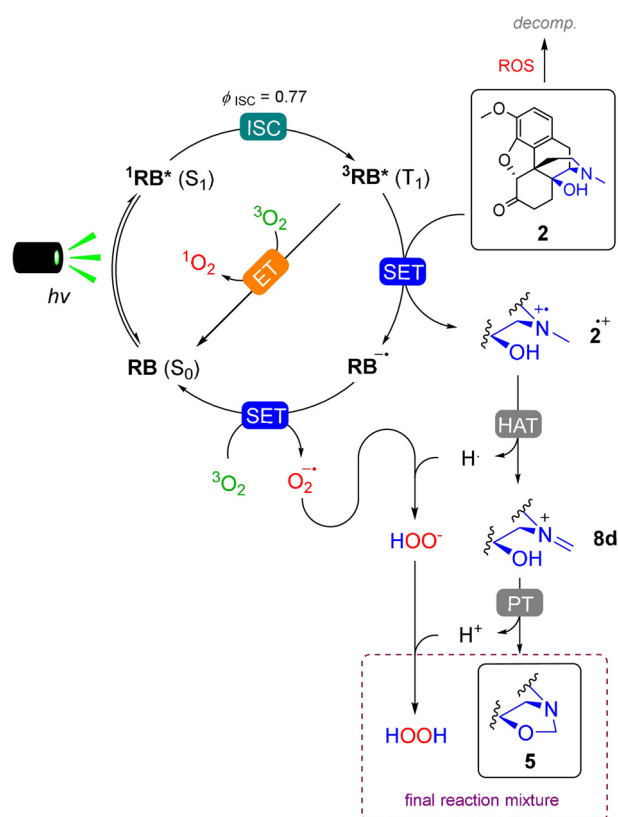


**Figure 1.** Stern–Volmer quenching experiment of RB using **2** (OC) as a quencher in different solvents ( $T = 21^\circ\text{C}$ ,  $[\text{RB}] = 1 \mu\text{mol L}^{-1}$ ). Viscosity of the solvents:  $\eta$  (MeOH) = 0.5838 MPa s,  $\eta$  (EtOH) = 1.170 MPa s and  $\eta$  (*n*-PrOH) = 2.125 MPa s.

Additional control experiments in deuterated solvents ( $\text{CDCl}_3$  and  $\text{CD}_3\text{OD}$ ) excluded the direct participation of  $^1\text{O}_2$  in side reactions, as no significant changes in the amount of side-products could be observed (the life time of  $^1\text{O}_2$  is longer in deuterated solvents) (see Figure S13 in the Supporting Information). Yet, photochemically generated ROS were responsible both for catalyst bleaching and decreased selectivities. A fast photochemical bleaching of RB could be observed only in the presence of both  $\text{O}_2$  and a tertiary amine, implying the potential formation of ROS during the photocatalytic cycle (see Figure S15 in Supporting Information). Hydrogen peroxide is a common ROS encountered in photooxidations. When  $\text{H}_2\text{O}_2$  was added to the reaction mixture as additive, formation of side products and low product yields were observed (see Figure S16–S17 in Supporting Information). Gratifyingly, degradation of **5** was determined to be comparatively slow (see Figure S14). The rate of degradation of **5** was approximately 30 times slower than its formation under the reaction conditions, thus explaining the good selectivities achieved. Additionally, these results also suggested that an immediate quench of  $\text{H}_2\text{O}_2$  after the reaction (before workup) could be essential in

order to obtain high yields, as observed experimentally (vide infra).

Based on the experiments described above, an overall reaction mechanism was formulated (Scheme 2). The reaction pathway starts with excitation of RB to its singlet state ( $^1\text{RB}^*$ ), which is then converted to the triplet state ( $^3\text{RB}^*$ ). Oxycodone (**2**) undergoes an electron transfer with the triplet state of RB. The resulting radical cation ( $2^{\cdot+}$ ) is then converted to iminium cation **8d** after the hydrogen-atom transfer (HAT) with the radical superoxide anion ( $\text{O}_2^{\cdot-}$ ) generated during the catalyst turnover. Then, **8d** undergoes an intramolecular nucleophilic addition to afford **5** and a stoichiometric amount of  $\text{H}_2\text{O}_2$ . This mechanism is in agreement with the typical iminium cation generation pathways by means of photoredox catalysis.<sup>[29]</sup>



**Scheme 2.** Suggested reaction mechanism.

### Optimization in flow

N-Demethylation of oxycodone (**2**) has often been carried out in high-boiling polar aprotic solvents, such as DMF, DMAc, and DMSO (b.p. >  $150^\circ\text{C}$ ).<sup>[18–20]</sup> To enable a more sustainable process, in this work we sought for a greener solvent alternative.<sup>[30]</sup> After an extensive solvent screening, a 1:1 mixture of methanol (MeOH) and *n*-butyl acetate (*n*BuOAc, b.p. =  $126^\circ\text{C}$ ) was found to be able to dissolve **2** in 0.1 M concentration at  $40^\circ\text{C}$ , and also provided good results for the demethylation reaction (similar to DMAc or DMF, see the Supporting Information). Our initial flow experiments using a commercially available flow photoreactor (Corning Lab Photo Reactor)<sup>[31]</sup> were carried out using this solvent mixture. The continuous flow

setup (Figure 2a) consisted of two feeds: the solution and oxygen were introduced with constant flow rates ( $F_L = 0.9 \text{ mL min}^{-1}$ ,  $F_G = 2.1 \text{ mL}_N \text{ min}^{-1}$ ; 1 equiv  $\text{O}_2$ ) into the reactor, a glass microreactor plate (155 × 125 × 8 mm, 2.77 mL internal volume, temperature 40 °C) flanked by two LED panels. The system pressure was controlled by a back pressure regulator ( $p = 5 \text{ bar}$ ) at the outlet. The substrate solution (0.1 M **2** + 2 mol% RB) was introduced into the system using a sample loop (10 mL) heated to 50 °C through a six-way valve. The tubing between the injection loop and the flow plate was kept short to avoid cooling of the liquid mixture and potential clogging caused by crystallization of **2**.

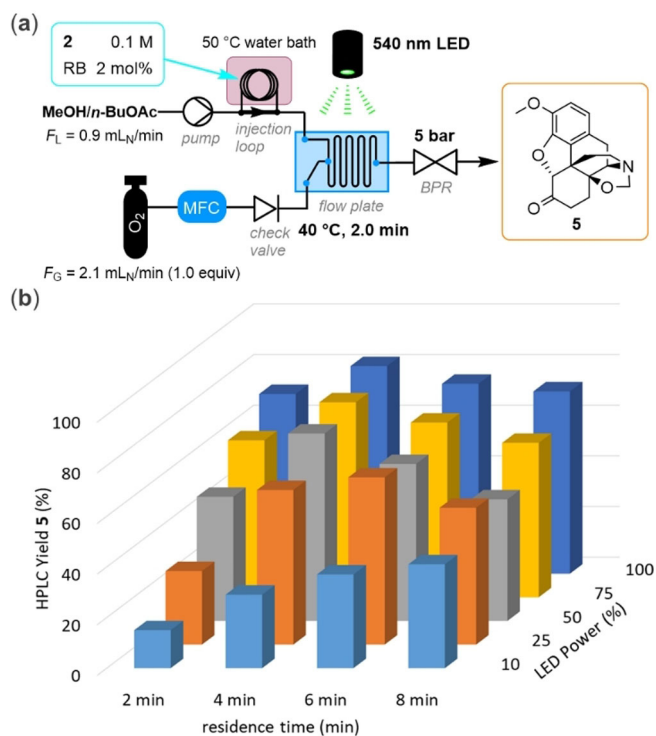


**Figure 2.** Flow setup for the N-demethylation of **2** and optimization of the residence time and relative irradiation power ( $P/P_{max}$ ).

Using green LEDs ( $\lambda = 540 \text{ nm}$ ) at their full power ( $P_{max} = 18.8 \text{ W}$ ), we achieved 90% conversion and 71% calibrated HPLC yield within 2.0 min residence time ( $t_R$ ). A second processing of the reaction mixture through the reactor under the same conditions provided 98% conversion of **2** and 82% HPLC yield of **5** (total residence time  $t_{R,tot} = 4.0 \text{ min}$ ). Then, several flow reactions under variable light irradiation power and residence time were carried out (Figure 2b). Best yields were achieved using the maximum power of the light source. Interestingly, an optimum value for the residence time (ca. 4 min) was clearly observed. Further prolonging the residence time led to the partial product decomposition by reaction of **5** with ROS.

To avoid the requirement of heating the substrate liquid feed to 50 °C and to ensure that no clogging of the system is caused by precipitation of **2** in the reactor during prolonged operation time, the solvent system was further refined. Using a ternary mixture of MeOH/MeCN/*n*BuOAc (1:1:1 vol.), sub-

strate **2** could be dissolved in a 0.1 M concentration at room temperature (20 °C). With this new solvent, N-demethylation of **2** was performed by using a liquid flow rate of  $0.5 \text{ mL}_N \text{ min}^{-1}$  and 6 bar backpressure. A conversion of 96 and 87% calibrated HPLC yield of **5** were obtained in a single pass ( $t_R = 3.5 \text{ min}$ ). Notably, the reaction temperature did not have a significant influence on the reaction outcome (Figure 3a), confirming the results already observed in batch. The catalyst (RB) loading could be reduced to 1 mol% without adverse effect. Upon further decrease of the catalyst loading (0.5 mol%), the conversion dropped (Figure 3b). In contrast, the use of EY as a photocatalyst resulted in lower conversions (<75%) even when with a catalyst loading of 4 mol% (Figure 3c).

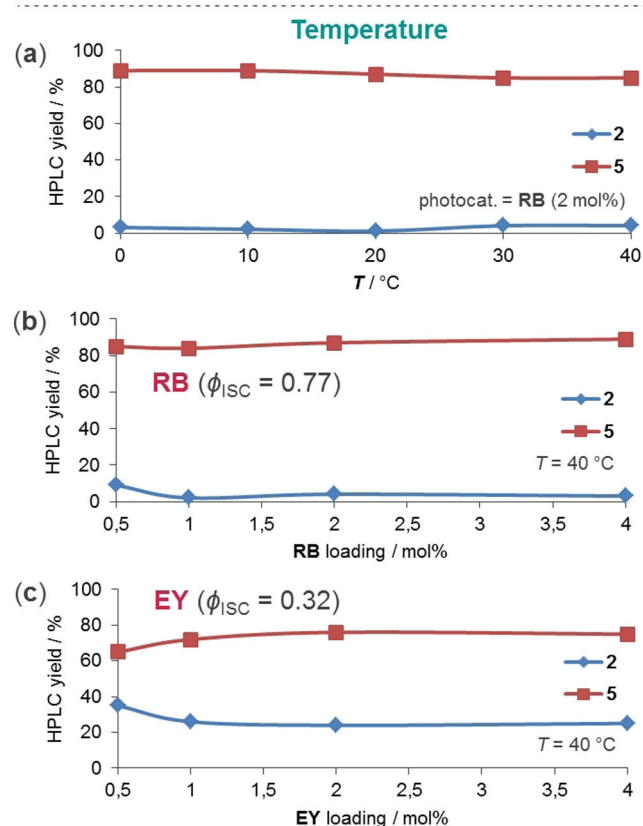
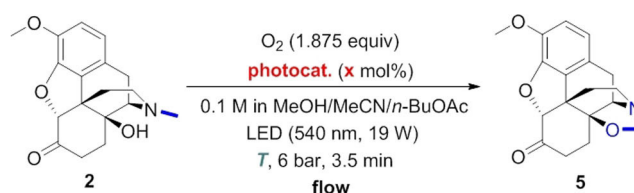


**Figure 3.** Influence of reaction temperature and catalyst loading in the continuous photochemical generation of **5**.

### Oxazolidine (**5**) hydrolysis and product isolation

Once the continuous flow photochemical generation of oxazolidine **5** had been optimized, we turned our attention to the generation of the target nor-compound **3**. The hydrolysis method developed in our previous research<sup>[18]</sup> consisted of

treating **5** with HCl (1 M, aq.) at 80 °C under reduced pressure (140 mbar) to enhance the elimination of formaldehyde from the reaction mixture. However, workup of the reaction mixture obtained after photolysis experiments at elevated temperatures provoked the formation of side-products, most probably due to the presence of ROS (mainly H<sub>2</sub>O<sub>2</sub>). For this reason we developed a novel workup protocol under atmospheric pressure. The crude photolysis mixture was stirred with two equivalents of sodium ascorbate (NaAsc) to quench the ROS and then was refluxed with a 3:1 mixture of 1 M aqueous HCl and ethanol for 2 h. The refluxing mixture was sparged with argon to facilitate elimination of the released formaldehyde byproduct. Using the optimized N-demethylation conditions in combination with this new hydrolysis procedure, noroxycodone (**3**) was prepared as its hydrochloride salt with good purity after an acid–base workup (Table 2, entries 1–2). The yield of **3** from the larger scale run is slightly higher, since the operation time at steady state is longer (Table 2, entry 2). For synthesis on a preparative scale (> 1 mmol), the substrate solution was delivered through the HPLC pump instead of a sample loop.<sup>[32]</sup> The stability of the flow system was demonstrated by a long run over 124 min (6.2 mmol scale) at a 20 °C reaction temperature (Table 2, entry 3). From the collected reaction mixture, noroxycodone hydrochloride (**3**·HCl) was isolated in 68% yield (1.4 g) after hydrolysis.

quenching of the triplet state of the catalyst (RB) with **2** plays an important role in the catalysis. Singlet oxygen does not contribute to the formation of **5**. The ROS generated during the reaction are responsible for the decomposition of the opiates, requiring a reductive quench afterwards. A scalable methodology has been achieved by translating the process to a continuous flow reactor. Under optimal conditions, oxazolidine **5** could be obtained in 87% HPLC yield after a 3.5 min residence time. Acidic hydrolysis of **5** furnished the desired nor-derivative **3** as its hydrochloride salt with 75% isolated yield. This photochemical approach avoids the use stoichiometric amounts of electrophiles, metal catalysts, or harsh reaction conditions (Scheme 1). In addition, the reaction can be performed under mild reaction conditions in a relatively benign solvent mixture.

## Experimental Section

### Photocatalytic N-demethylation of oxycodone (**2**) and H<sub>2</sub>O<sub>2</sub> quenching

Using the setup shown in Table 2, (reactor settings:  $F_L = 0.5 \text{ mL}_N \text{ min}^{-1}$ ,  $F_G = 2.1 \text{ mL}_N \text{ min}^{-1}$ ,  $T = 40 \text{ }^\circ\text{C}$ ,  $p = 6 \text{ bar}$ ), after warming of the light source and stabilization of the temperatures and pressure, a 0.1 M solution of oxycodone (**2**) and 2 mol% rose bengal (RB) in MeOH/MeCN/*n*BuOAc (1:1:1 vol.) was pumped into the reactor. When the steady state was reached, the reaction mixture was collected at the reactor outlet with a graduated cylinder. As soon as the collection was finished, the volume of the reaction mixture was recorded; the collected reaction mixture was transferred into a 100 mL three-necked flask and stirred with two equivalents of sodium ascorbate (NaAsc) over 16 h at room temperature in the dark.

### Hydrolysis of oxazolidine (**5**) and isolation of noroxycodone hydrochloride (**3**·HCl)

The reaction mixture after the NaAsc treatment (H<sub>2</sub>O<sub>2</sub> quenching) was evaporated to dryness at 45 °C in vacuo, and then refluxed with HCl (1 M, aq.)/ethanol (3:1 vol.) for 2 h while argon bubbling. The hydrolysis mixture was concentrated in vacuo over 10 min at 40 °C, 100 mbar, added with 5 mL HCl (1 M, aq.) and extracted with 2 × 30 mL CHCl<sub>3</sub>. The aqueous phase was collected and basified with 25% NH<sub>3</sub> solution to pH ≈ 10 and then extracted with 4 × 30 mL CHCl<sub>3</sub>. The combined organic phase was dried over anhydrous Na<sub>2</sub>SO<sub>4</sub>, filtered, and concentrated in vacuo. The residue was dissolved in 2 equiv HCl (1.25 M, MeOH solution), evaporated in vacuo to dryness, washed with 3 × 2 mL diethyl ether and dried in vacuo overnight at 40 °C affording noroxycodone hydrochloride (**3**·HCl) as a water-soluble yellowish solid.

## Acknowledgements

The CC FLOW Project (Austrian Research Promotion Agency FFG No. 862766) is funded through the Austrian COMET Program by the Austrian Federal Ministry of Transport, Innovation and Technology (BMVIT), the Austrian Federal Ministry of Science, Research and Economy (BMWFW), and by the State of Styria (Styrian Funding Agency SFG). The authors gratefully acknowledge Corning SAS for the generous loan of the Corning

**Table 2.** Preparative runs, workup and isolation.<sup>[a]</sup>

Entry	Scale [mmol]	$T$ [°C] <sup>[a]</sup>	Yield <b>3</b> ·HCl [%] <sup>[b]</sup>	Purity [%] <sup>[c]</sup>
1	1.0	40	70	94
2	2.2	40	75	94
3	6.2	20	68	88 <sup>[d]</sup>

[a] Temperature of the photochemical step. [b] Isolated yield. [c] Determined by HPLC peak area integration. [d] 93% purity obtained after acid–base work-up (see the Supporting Information).

## Conclusions

We have developed a photocatalytic procedure for the N-demethylation of oxycodone (**2**) using molecular oxygen as the terminal oxidant and rose bengal as an inexpensive, metal free organophotocatalyst. Mechanistic studies revealed that

Advanced-Flow Lab Photo Reactor used in this study. We are also thank Prof. Dr. Till Opatz for his informative suggestions during this research.

## Conflict of interest

The authors declare no conflict of interest.

**Keywords:** continuous-flow · gas/liquid reaction · N-demethylation · opioid · photocatalysis

- [1] a) S. Berenyi, C. Csutoras, A. Sipos, *Curr. Med. Chem.* **2009**, *16*, 3215–3242; b) A. F. Casy, R. T. Parfitt, *Opioid Analgesics*; Plenum Press: New York and London, **1986**; c) H. Nagase, Ed. *Chemistry of Opioids*; Springer: Heidelberg, **2011**.
- [2] a) N. Sharghi, I. Lalezari, *Nature* **1967**, *213*, 1244; b) J. W. Fairbairn, *Planta Medica* **1976**, *29*, 26–32; c) L. E. Craker, J. E. Simon, Eds. *Herbs, Spices, and Medicinal Plants: Recent Advances in Botany, Horticulture, and Pharmacology* Vol. II, . Haworth Press Inc., Binghamton NY, **1991**; d) I. Schönfelder, P. Schönfelder, *Der Kosmos Heilpflanzenführer: Über 600 Heil- und Giftpflanzen Europas*, 4th Ed.; Franckh Kosmos Verlag: Stuttgart, **2019**.
- [3] a) A. Ordóñez Gallego, M. G. Baron, E. E. Arranz, *Clin. Transl. Oncol.* **2007**, *9*, 298–307; b) J. Riley, E. Eisenberg, G. Müller-Schwefe, A. M. Drewes, L. Arendt-Nielsen, *Curr. Med. Res. Opin.* **2008**, *24*, 175–192; c) S. J. King, C. Reid, K. Forbes, G. Hanks, *Palliat. Med.* **2011**, *25*, 454–470.
- [4] a) United Nations Office on Drugs and Crime, World Health Organization, *Opioid overdose: preventing and reducing opioid overdose mortality*, United Nations, **2013**; b) G. Willyard, *Nature* **2019**, *573*, S17–S19.
- [5] M. S. Sadove, R. C. Balagot, S. Hatano, E. A. Jobgen, *JAMA J. Am. Med. Assoc.* **1963**, *183*, 666–668.
- [6] a) A. K. Clark, C. M. Wilder, E. L. Winstanley, *J. Addict. Med.* **2014**, *8*, 153–163; b) J. M. Chamberlain, B. L. Klein, *Am. J. Emerg. Med.* **1994**, *12*, 650–660.
- [7] World Health Organization, *World Health Organization Model List of Essential Medicines*, 21<sup>st</sup> List, United Nations, **2019**.
- [8] For the synthesis of Naloxone from oripavine, see: a) R. J. Kupper, US7939543, 10 May, **2011**; b) J. R. Giguere, H. A. Reisch, S. Sandoval, J. L. Stymiest, US8921556, 30 December, **2014**.
- [9] a) J. D. Phillipson, A. Scutt, A. Baytop, N. Özhatay, G. Sariyar, *Planta Medica* **1981**, *43*, 261–271; b) A. Coop, J. W. Lewis, K. C. Rice, *J. Org. Chem.* **1996**, *61*, 6774.
- [10] For the synthesis of Naloxone from thebaine, see: a) Z. Fang, J. Wang, W. Jiang, L. Zhang, R. Yu, D. Zhao, CN104230945 A, 24 December, **2014**; b) Y. Zheng, M. Lu, X. Wang, W. Sheng, Z. Qiu, *Fudan Xuebao, Yixueban* **2007**, *34*, 888–890; c) J. Cardot, W.-C. Zhang, US9701687, 11 July, **2017**; d) M. Conza, V. Lellek, H. Zinser, US9701688, 11 July, **2017**.
- [11] L. Werner, M. Wernerova, A. Machara, M. A. Endoma-Arias, J. Duchek, D. R. Adams, D. P. Cox, T. Hudlický, *Adv. Synth. Catal.* **2012**, *354*, 2706–2712.
- [12] S. Thavaneswaran, K. McCamley, P. J. Scammells, *Nat. Prod. Commun.* **2006**, *1*, 885–897.
- [13] For the N-demethylation using chloroformate, see: a) A. Kimishima, C. J. Wenthur, B. Zhou, K. D. Janda, *ACS Chem. Biol.* **2017**, *12*, 36–0; b) R. A. Olofson, J. T. Martz, J. P. Senet, M. Piteau, T. Malfroot, *J. Org. Chem.* **1984**, *49*, 2081–2082; c) M. A. Schwartz, R. A. Wallace, *J. Med. Chem.* **1981**, *24*, 1525–1528.
- [14] For the N-demethylation using BrCN, see: a) A. Machara, M. A. A. Endoma-Arias, I. Císařova, D. P. Cox, T. Hudlický, *Synthesis* **2016**, *48*, 1803–1813; b) B. R. Selfridge, X. Wang, Y. Zhang, H. Yin, P. M. Grace, L. R. Watkins, A. E. Jacobson, K. C. Rice, *J. Med. Chem.* **2015**, *58*, 5038–5052.
- [15] For the N-demethylation using H<sub>2</sub>O<sub>2</sub>, see: a) D. D. Do Pham, G. F. Kelso, Y. Yang, M. T. Hearn, *Green Chem.* **2014**, *16*, 1399–1409; b) G. B. Kok, P. J. Scammells, *Bioorg. Med. Chem. Lett.* **2010**, *20*, 4499–4502; c) Z. Dong, P. J. Scammells, *J. Org. Chem.* **2007**, *72*, 9881–9885; d) K. McCamley, J. A. Ripper, R. D. Singer, P. J. Scammells, *J. Org. Chem.* **2003**, *68*, 9847–9850.
- [16] For the N-demethylation using O<sub>2</sub> and Pd, see: a) R. J. Carroll, H. Leisch, E. Scocchera, T. Hudlický, D. P. Cox, *Adv. Synth. Catal.* **2008**, *350*, 2984–2992; b) A. Machara, L. Werner, M. A. Endoma-Arias, D. P. Cox, T. Hudlický, *Adv. Synth. Catal.* **2012**, *354*, 613–626.
- [17] A. Machara, D. P. Cox, T. Hudlický, *Adv. Synth. Catal.* **2012**, *354*, 2713–2718.
- [18] B. Gutmann, U. Weigl, D. P. Cox, C. O. Kappe, *Chem. Eur. J.* **2016**, *22*, 10393–10398.
- [19] B. Gutmann, D. Cantillo, U. Weigl, D. P. Cox, C. O. Kappe, *Eur. J. Org. Chem.* **2017**, 914–927.
- [20] B. Gutmann, P. Elsner, D. P. Cox, U. Weigl, D. M. Roberge, C. O. Kappe, *ACS Sustainable Chem. Eng.* **2016**, *4*, 6048–6061.
- [21] J. A. Ripper, E. R. Tiekink, P. J. Scammells, *Bioorg. Med. Chem. Lett.* **2001**, *11*, 443–445.
- [22] a) J. W. Beatty, C. R. Stephenson, *Acc. Chem. Res.* **2015**, *48*, 1474–1484; b) G. Wu, Y. Li, X. Yu, Y. Gao, H. Chen, *Adv. Synth. Catal.* **2017**, *359*, 687–692.
- [23] a) P. Sobieszuk, J. Aubin, R. Pohorecki, *Chem. Eng. Technol.* **2012**, *35*, 1346–1358; b) G. N. Doku, W. Verboom, D. N. Reinhoudt, A. van den Berg, *Tetrahedron* **2005**, *61*, 2733–2742.
- [24] a) D. Cambié, C. Bottecchia, N. J. Straathof, V. Hessel, T. Noël, *Chem. Rev.* **2016**, *116*, 10276–10341; b) Y. Su, N. J. Straathof, V. Hessel, T. Noël, *Chem. Eur. J.* **2014**, *20*, 10562–10589; c) K. Gilmore, P. H. Seeberger, *Chem. Rec.* **2014**, *14*, 410–418; d) L. D. Elliott, J. P. Knowles, P. J. Koovits, K. G. Maskill, M. J. Ralph, G. Lejeune, L. J. Edwards, R. I. Robinson, I. R. Clemens, B. Cox, D. D. Pascoe, *Chem. Eur. J.* **2014**, *20*, 15226–15232; e) E. M. Schuster, P. Wipf, *Isr. J. Chem.* **2014**, *54*, 361–370.
- [25] C. A. Hone, D. Roberge, C. O. Kappe, *ChemSusChem* **2017**, *10*, 32–41.
- [26] T. Y. Shang, L. H. Lu, Z. Cao, Y. Liu, W. M. He, B. Yu, *Chem. Commun.* **2019**, *55*, 5408–5419.
- [27] A. P. Darmanyan, *Chem. Phys. Lett.* **1984**, *110*, 89–94.
- [28] R. C. Kanner, C. S. Foote, *J. Am. Chem. Soc.* **1992**, *114*, 678–681.
- [29] a) N. A. Romero, D. A. Nicewicz, *Chem. Rev.* **2016**, *116*, 10075–10166; b) M. H. Shaw, J. Twilton, D. W. C. MacMillan, *J. Org. Chem.* **2016**, *81*, 6898–6926; c) J. W. Tucker, C. R. J. Stephenson, *J. Org. Chem.* **2012**, *77*, 1617–1622.
- [30] C. J. Clarke, W.-C. Tu, O. Levers, A. Bröhl, J. P. Hallett, *Chem. Rev.* **2018**, *118*, 747–800.
- [31] Y. Chen, O. de Frutos, C. Mateos, J. A. Rincon, D. Cantillo, C. O. Kappe, *ChemPhotoChem* **2018**, *2*, 906–912.
- [32] This work was carried out with a 2.77 mL reactor. It should be noted that the commercial platform utilized can be readily scaled up even for gas liquid mixtures by simply using larger volume plates: N. Emmanuel, C. Mendoza, M. Winter, Horn, C. A. Vizza, L. Dreesen, B. Heinrichs, J.-C. M. Monbaliu, *Org. Process Res. Dev.* **2017**, *21*, 1435–1438.

Manuscript received: December 6, 2019

Revised manuscript received: January 2, 2020

Accepted manuscript online: January 3, 2020

Version of record online: February 18, 2020